



Charge and heat transfer of the Ti_3AlC_2 MAX phase

R. V. Vovk^{1,2} · G. Ya. Khadzhai¹ · T. A. Prikhna³ · E. S. Gevorkyan² · M. V. Kislitsa² · A. L. Soloviev⁴ · I. L. Goulatis¹ · A. Chroneos^{5,6}

Received: 9 March 2018 / Accepted: 5 May 2018
© The Author(s) 2018

Abstract

The electrical and thermal conductivity of the sample containing 97% by volume of the Ti_3AlC_2 MAX phase and 3% volume TiC was experimentally studied in the temperature range 15–300 K. The temperature dependence of the electrical resistance is approximated by a relation that takes into account the scattering of electrons by phonons and defects. The temperature dependence of the thermal conductivity shows a maximum at about 75 K. In the region of elastic scattering of electrons, the phonon and electron heat transfer are separated. With increasing temperature, the fraction of phonon heat transfer decreases from ~90% at low temperatures to ~40% near room temperature.

1 Introduction

Synthesizing and studying new functional materials that can be employed in multiple technological applications [1–5] is a key direction of solid state physics. One of the most promising classes of such compounds are the so-called MAX phases [1–3] (with the general formula $\text{M}_{n+1}\text{AX}_n$, where M is the transition material, A is the element of the III- or IV-subgroup of the periodic system, and X is carbon or nitrogen). Strong M–X bonds, weaker M–A bonds associated with the nanolayered nature of the structure provide a unique combination of metal and ceramic properties for these substances [6]. The layered perovskite-like unit cell

leads to the nanolaminated structure of the MAX-phase based materials which in turn gives the possibility of grains local deformation in the zone of stress concentration without their macroscopic destruction. These compounds have a unique combination of metallic and ceramic properties, such as high hardness, high refractive index, elasticity, good thermal and electrical conductivity. The latter is crucial for the successful application of these materials in modern micro- and nanoelectronics, switching devices, and energy [7–9]. For example, recent studies have examined the application of MAX phases in nuclear applications [7] and the use of the 2D MXenes (synthesized from the MAX phases) for electromagnetic interference shielding [8].

The study of the mechanisms of electrical and heat transfer in these compounds is a tool for testing the adequacy of the corresponding theoretical models and facilitates the determination of empirical ways of improving their technological characteristics. In the present study we have investigated the thermal and electrical conductivity of the Ti_3AlC_2 MAX phase in the temperature range of 15–300 K.

2 Experimental methods and techniques

2.1 Sample preparation

The sample of the MAX phase Ti_3AlC_2 were fabricated using Spark Plasma Sintering (SPS) technology by sintering the initial powder in a hot pressing plant, while simultaneously passing a current of the order of several kA along the pressing

✉ A. Chroneos
alexander.chroneos@imperial.ac.uk

¹ V.N. Karazin Kharkiv National University, 4 Svoboda sq., Kharkiv 61022, Ukraine

² Ukrainian State University of Railway Transport, 7 Feuerbach sq., Kharkiv 61050, Ukraine

³ V. Bakul Institute for Superhard Materials of the National Academy of Sciences of Ukraine, 2 Avtozavodska St., Kyiv 04074, Ukraine

⁴ B. Verkin Institute for Low Temperature Physics and Engineering of the National Academy of Sciences of Ukraine, 47 Nauky Ave., Kharkiv 61103, Ukraine

⁵ Faculty of Engineering, Environment and Computing, Coventry University, Priory Street, Coventry CV1 5FB, UK

⁶ Department of Materials, Imperial College London, London SW7 2AZ, UK

axis through the graphite mold and the powder itself, which resulted both, the heating and the cleaning of the surface of the powder particles, due to microdischarges on their surface.

Figure 1 shows a diffraction pattern from the investigated sample—pressing temperature $T = 1350$ °C, pressure $P = 30$ MPa, holding time 30 min. In Table 1 we report the data characterizing the material. The predominant phase is Ti_3AlC_2 (volume fraction $\approx 97\%$); whereas the volume fraction of TiC is $\approx 3\%$. The lattice parameters are close to [10].

2.2 Measurements

The electrical resistivity of the sample was measured using the standard four-probe technique. The thermal conductivity was measured by the uniaxial stationary heat flow method. The temperature drop along the sample was measured with a copper-constantan thermocouple. The electrical contacts in the electrical resistivity measurements and the heat contacts in the thermal conductivity measurements were located in the same positions.

3 Results and discussion

The experimental results for the electrical resistivity of the investigated sample in the interval 15–320 K are shown in Fig. 2. Notably, the resistivity values obtained are characteristic for alloys with defects, as evidenced by the ratio $RRR = \rho(300 \text{ K})/\rho(4.2 \text{ K}) \approx 1.9$.

In the temperature range investigated, the electric resistance of the sample is due to the scattering of charge carriers by phonons and defects:

$$\rho(T) = \rho_0 + \rho_{ph}(T). \quad (1)$$

where ρ_0 is the residual resistivity, caused by scattering of charge carriers by defects. The scattering of charge carriers by phonons, $\rho_{ph}(T)$, can be approximated with a high degree of accuracy by the formula [14]:

$$\rho_{ph}(T) = C_3 \left(\frac{T}{\theta}\right)^3 \cdot \int_0^{\theta/T} \frac{x^3 e^x}{(e^x - 1)^2} dx, \quad (2)$$

Table 1 The phase composition of a sample obtained by the electroconsolidation method

	Ti_3AlC_2	TiC
Density (g/cm^3)	4.24	4.93
Volume fraction (%)	96.65	3.35
Lattice parameters		
a (Å)	3.0717	4.315
c (Å)	18.547	

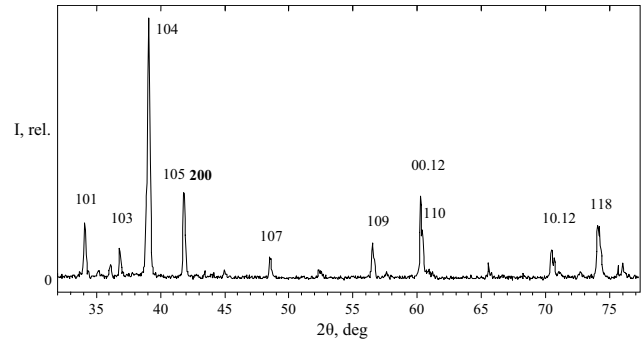


Fig. 1 The fragment of X-ray diffraction pattern with Miller index (bold for TiC) of the MAX phase Ti_3AlC_2 obtained by hot pressing electroconsolidation method

where θ is the Debye temperature; C_3 is a fitting coefficient.

The minimum error of approximation after (1, 2), $\Delta\rho/\rho \approx 0.5\%$, was achieved at the parameters' values, shown in Table 2. In the same table, we compare the parameters of a similar fit for the data [11, 12] for Ti_3AlC_2 , [13] for TiC and our data for Ti.

From Fig. 2 and Table 2 it is shown that ρ_0 for Ti_3AlC_2 and TiC is much larger than for Ti. Because the residual resistivity ρ_0 is caused by scattering of charge carriers by defects, it is deduced that the MAX-phase and titanium carbide contain significantly more defects than metallic Ti. Therefore, at low temperatures, where the main role is played by the scattering of charge carriers by defects, $\rho^{\text{Ti}} < \rho^{\text{Ti}_3\text{AlC}_2}$. At sufficiently high temperatures $\rho^{\text{Ti}} > \rho^{\text{Ti}_3\text{AlC}_2}$ due to more intensive scattering of charge carriers by phonons ($C_3^{\text{Ti}} > C_3^{\text{Ti}_3\text{AlC}_2}$).

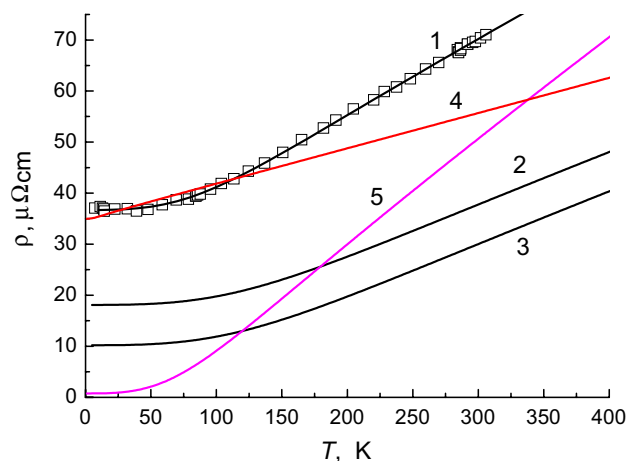
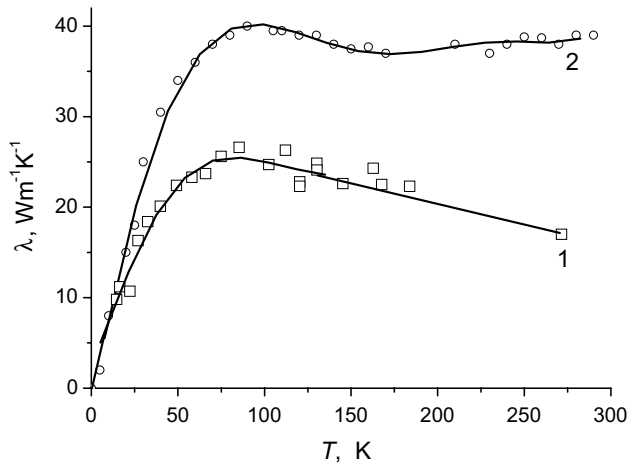


Fig. 2 The temperature dependencies of the resistivity: 1—our data, 2—[11], 3—[12] for Ti_3AlC_2 ; 4—data [13] for TiC; 5—our data for Ti. The points are the experiment, the lines are approximations by Eq. (1, 2)

Table 2 The fitting parameters according to relations (1, 2) of the experimental data for $\rho(T)$

	$\rho_0, \mu\Omega \text{ cm}$	$\theta, \text{ K}$	$C_3, \mu\Omega \text{ cm}$	RRR
Experiment	36.7	612	161	1.9
Data according to [11]	18.1	876	158	2.1
Data according to [12]	10.2	873	159	3
TiC [13]	36	—	—	1.5
Ti	0.76	500	186	67

**Fig. 3** Temperature dependences of thermal conductivity, $\lambda(T)$, of Ti_3AlC_2 : 1—our data, 2—[12]. The points are for the experiment, the lines are drawn “to the eye”

The values of the Debye temperature for Ti_3AlC_2 decrease with increasing ρ_0 . The fact is that the comparatively high values of θ are due to significant anisotropy of Ti_3AlC_2 [12], but the defects make the phonon spectrum more isotropic, thereby reducing θ . The fitting coefficient C_3 for Ti_3AlC_2 is very weakly dependent on the concentration of defects.

The temperature dependence of the thermal conductivity of the sample shows a maximum at $T_m \approx 85 \text{ K}$ (refer to Fig. 3). We note that the maximum of thermal conductivity exists both in the case of heat transfer by charge carriers and in the case of heat transfer by phonons if the structure of the sample is quite perfect. Defects shift both maxima to the right and reduce their heights. However, in our case the higher maximum (refer to Fig. 3, curve 2) is located to the right of the lower maximum. This indicates the presence of two mechanisms of heat transfer—by charge carriers and by phonons, comparable in efficiency. The evolution of the total maximum is due to the fact that the defects have different effects on each of the maxima.

In the region of charge carriers' elastic scattering is performed the Wiedemann–Franz law [15]:

$$\lambda_e \approx L_0 T / \rho \quad (3)$$

here, λ_e is the thermal conductivity, which characterizes the transfer of heat by charge carriers; $L_0 = 2.45 \times 10^{-8} \text{ W } \Omega \text{ K}^{-2}$ is the Sommerfeld value of the Lorentz number.

The elastic scattering conditions are satisfied at low temperatures ($T \ll \theta$), where the elastic scattering of charge carriers by defects predominates. Here $\rho(T) \approx \rho_0$, $\lambda_e = L_0 T / \rho_0$. At $T \approx 15 \text{ K}$ this gives $\lambda_e \approx 1 \text{ W m}^{-1} \text{ K}^{-1}$. Comparing this value with the experimental value of low-temperature thermal conductivity ($\approx 10 \text{ W m}^{-1} \text{ K}^{-1}$) shows that at low temperatures the 90% of the heat is transferred by phonons.

The elastic scattering conditions are satisfied too at sufficiently high temperatures ($T > \theta$), where the elastic scattering of charge carriers by phonons predominates. Here $\rho(T) \approx \rho_0(1 + \alpha T)$ and $\lambda_e = L_0 T / \rho(T) \approx \text{const}$. The λ_e value estimated from relation (3) is $\lambda_e \approx 10 \text{ W m}^{-1} \text{ K}^{-1}$ for $T = 300 \text{ K}$, which is about 60% of the experimental value of thermal conductivity at this temperature, that is, phonons part is about 40% of the transferred heat. A specific role in this may be played by specific mechanisms of quasiparticle scattering [16–21], due to the presence of structural and kinematic anisotropy in the system.

Thus, the fraction of phonon heat transfer in the MAX phase Ti_3AlC_2 decreases by increasing temperature, since the charge carriers thermal conductivity at high temperatures is constant, and the phonon thermal conductivity decreases as $1/T$.

4 Conclusions

The electrical and thermal conductivity studies of the MAX phase Ti_3AlC_2 sample showed that the investigated MAX phase contains a large number of defects, which leads to a large value of the residual resistance and reduces the Debye temperature, probably due to isotropization. Heat in the sample is transferred both by phonons and charge carriers, with phonon thermal conductivity predominating at low temperatures, but decreases with increasing temperature.

Open Access This article is distributed under the terms of the Creative Commons Attribution 4.0 International License (<http://creativecommons.org/licenses/by/4.0/>), which permits unrestricted use, distribution, and reproduction in any medium, provided you give appropriate credit to the original author(s) and the source, provide a link to the Creative Commons license, and indicate if changes were made.

References

1. M.A. Hadi, R.V. Vovk, A. Chroneos, J. Mater. Sci. Mater. Electron. **27**, 11925–11933 (2016)
2. E.N. Sgourou, Y. Panayiotatos, R.V. Vovk, A. Chroneos, Appl. Sci. **7**, 674 (2017)

3. T.A. Prikhna, A.V. Starostina, I.A. Petrusha, S.A. Ivakhnenko, A.I. Borimskii, Yu.D. Filatov, M.G. Loshak, M.A. Serga, V.N. Tkach, V.Z. Turkevich, V.B. Sverdun, S.A. Klimenko, D.V. Turkevich, S.N. Dub, T.V. Basyuk, M.V. Karpets, V.E. Moshchil', A.V. Kozyrev, G.D. Il'nitskaya, V.V. Kovylyayev, D. Lizkendorf. T. Cabiosh, P. Chartier, *J. Superhard Mater.* **36**, 9–17 (2014)
4. M. Dahlqvist, B. Alling, J. Rosén., *Phys. Rev. B* **81**, 220102 (2010). R)
5. M.A. Hadi, M. Roknuzzaman, A. Chroneos, S.H. Naqib, A.K.M.A. Islam, R.V. Vovk, K. Ostrikov, *Comp. Mater. Sci.* **137**, 318 (2017)
6. M. Barsoum, *Prog. Solid St. Chem.* **28**, 201–228 (2000)
7. D. Horlait, S.C. Middleburgh, A. Chroneos, W.E. Lee, *Sci. Rep.* **6**, 18829 (2016)
8. F. Shahzad, M. Alhabeab, C.B. Hatter, B. Anasori, S.M. Hong, C.M. Koo, Y. Gogotsi, *Science* **353**, 1137–1140 (2016)
9. Y. Tong, M. He, Y. Zhou, X. Zhong, L. Fan, T. Huang, Q. Liao, Y. Wang, *Appl. Surf. Sci.* **434**, 28–293 (2018)
10. Z.M. Sun, *Inter. Mater. Rev.* **56**, 143–166 (2011)
11. M.W. Barsoum, *MAX Phases, Properties of Machinable Ternary Carbides and Nitrides. First Edition* (Wiley, Hoboken, 2013) p. 421
12. X.H. Wang, Y.C. Zhou, *Acta Mater.* **50**, 3141 (2002)
13. S.N. L'vov, V.F. Nemchenko, T.Ya. Kosolapova, G.V. Samsonov, *Dokl. AS USSR* **157**, 408–411 (1964)
14. L. Colquitt, *J. Appl. Phys.* **36**, 2454 (1965)
15. R. Berman, *Thermal Conduction of Solids* (Clarendon Press, Oxford, 1976)
16. O.V. Dobrovolskiy, V.V. Sosedkin, R. Sachser, V.A. Shklovskij, R.V. Vovk, M. Huth, *J. Supercond. Nov. Magn.* **30**, 735–741 (2017)
17. P.G. Curran, V.V. Khotkevych, S.J. Bending, A.S. Gibbs, S.L. Lee, A.P. Mackenzie, *Phys. Rev. B* **84**, 104507 (2011)
18. A.L. Solovyov, L.V. Omelchenko, V.B. Stepanov, R.V. Vovk, H.-U. Habermeier, P. Przyslupski, K. Rogacki, *Phys. Rev. B* **94**, 224505 (2016)
19. V.M. Apalkov, M.E. Portnoi, *Phys. Rev. B* **65**, 125310 (2002)
20. O.V. Dobrovolskiy, M. Huth, V.A. Shklovskij, R.V. Vovk, *Sci. Rep.* **7**, 13740 (2017)
21. I.N. Adamenko, K.E. Nemchenko, V.I. Tsyganok, A.I. Chervanov. *Low Temp. Phys.* **20**, 498 (1994)